communications materials

ARTICLE

https://doi.org/10.1038/s43246-022-00309-4 OPEN

Extracellular matrix-inspired hydrogel of hyaluronan and gelatin crosslinked via a Link module with a transglutaminase reactive sequence

Masashi Okawa [1], Aki Tanabe[1], Seiichi Ohta[1,2], Satoru Nagatoishi [3], Kouhei Tsumoto[1,3] & Taichi Ito [1,2,4]✉

The extracellular matrix (ECM) is a natural scaffold of cells in the body. It has a complex structure comprising various proteins, such as collagen and hyaladherins, and polysaccharides such as hyaluronan (HA). Here, inspired by the crosslinked ECM structure, we design a genetically engineered Link module—LinkCFQ—by fusing a microbial transglutaminase (MTG)-reactive tag to the Link module, an HA-binding domain of tumor necrosis factor-stimulated gene-6. Although the HA-specific binding property of the Link module is preserved, LinkCFQ demonstrates excellent MTG reactivity with various proteins. Furthermore, an ECM-inspired hydrogel is fabricated from an HA–gelatin mixture crosslinked via HA/Link module interaction and MTG-catalyzed isopeptide bond formation in LinkCFQ. Cell culture and mouse experiments confirm the hydrogel's biocompatibility and degradability. Our findings provide insights into the design of biomaterials and proteins for tissue engineering, regenerative medicine, drug discovery and delivery, disease models, biofabrication, and medical devices.

[1] Department of Bioengineering, The University of Tokyo, Tokyo 113-8656, Japan. [2] Department of Chemical System Engineering, The University of Tokyo, Tokyo 113-8656, Japan. [3] The Institute of Medical Science, The University of Tokyo, Tokyo 108-8639, Japan. [4] Center for Disease Biology and Integrative Medicine, The University of Tokyo, Tokyo 113-0033, Japan. ✉email: taichi@m.u-tokyo.ac.jp

The functions of bioinspired materials have been considerably advanced by faithfully mimicking the structural templates of nature. For example, materials inspired by fish scales[1] and gecko adhesive surfaces[2] exhibit outstanding properties. In tissue engineering and regenerative medicine, various materials used for cell scaffolds have been studied; these are predominantly synthetic polymers such as polyethylene glycol and poly lactic acid[3,4] and biopolymers such as collagen[5], hyaluronic acid[6], and alginate[7,8]. In particular, hydrogels are an attractive option for tissue engineering because the natural scaffold in the human body is a hydrogel known as the extracellular matrix (ECM)[9]. The ECM has a complex structure comprising proteins and polysaccharides and contains intrinsic biochemical and mechanical cues that regulate cellular phenotype and function during development, homeostasis, and injury response[10]. Recently, with an improved understanding of the biological and biochemical properties of the ECM, ECM-inspired and/or -mimetic hydrogels have garnered considerable attention in the field of biomedical engineering and for use as biomaterials with superior properties[11–14].

Hyaluronan (HA), a major component of the ECM, is a non-sulfated glycosaminoglycan comprising repeated units of the polymeric disaccharides D-glucuronic acid and *N*-acetyl-D-glucosamine. HA is ubiquitous in vertebrates and present in some pathogenic bacteria[15,16]. In humans, HA play diverse biological roles as a structural component as well as a hydrated matrix for cell division, migration, and activation[9]. Such diversity results from a large number of HA-binding proteins (often termed hyaladherins)[17]. Many hyaladherins possess a common structural HA-binding domain of ca. 100 amino acids in length, known as a Link module. Proteoglycans such as aggrecan and versican contain two contiguous Link modules in their G1 domains and form huge, Link–protein-stabilized complexes with HA. Recent studies have implied that tumor necrosis factor-stimulated gene-6 (TSG-6)–mediated HA crosslinking via its Link module would be of great importance in the formation of HA-rich provisional matrices during wound healing[18,19]. However, although the Link module appears to be a key component in the ECM structure, to the best of our knowledge, no biomaterial has previously been designed based on the natural HA/Link module interaction[20,21].

Gelatins[9] are extracted from raw materials such as pig skin or bovine hide and are degraded collagen, which is another major component of the ECM. In vertebrates, a total of 28 genetic varieties of collagens have been discovered thus far[22]. Most collagen molecules form a triple-stranded helix[23], the structure of which is also preserved in bacteria[24]. During collagen synthesis, collagen fibrils are bundled together[25] and further crosslinked via lysyl oxidases (LOX) to strengthen the structural integrity of the tissue[26,27]. During wound healing, various ECM-modifying proteins are secreted by peripheral cells to promote ECM remodeling[28]. Transglutaminases (TG) such as TG2 and FXIII catalyze the crosslinking of collagen via the formation of highly stable ε(γ-glutamyl) lysine bonds called isopeptide bonds[27,29,30]. Enzymatic processing is a key method used for controlling the ECM structure and functions in nature. Microbial transglutaminase (MTG) has been well studied[31] for its reaction mechanism, biocompatibility, and easy conjugation ability, which are similar to those of the TGs in nature. Recently, a highly MTG-reactive tag was screened as a versatile protein functionalization linker for biomedical applications[32,33].

In the present study, inspired by natural ECM, we designed a genetically engineered Link module, LinkCFQ, by fusing an MTG-reactive tag to the Link module from tumor necrosis factor-stimulated gene-6 (TSG-6). We used low temperature and the molecular chaperone coexpression system to express LinkCFQ (soluble form) in *Escherichia coli* and purify it successfully. Although the physicochemical properties of the Link module were preserved, particularly the HA-specific binding property, LinkCFQ demonstrated excellent MTG reactivity with various proteins, forming Link–protein conjugates. To the best of our knowledge, this study is the first to fabricate an ECM-inspired hydrogel from a mixture of HA and gelatin via HA/Link module crosslinking and TG-catalyzed isopeptide bond formation of LinkCFQ. Furthermore, cell culture and animal experiments demonstrated that the hydrogel is biocompatible and degradable.

Results

Physicochemical properties of LinkCFQ. LinkCFQ was expressed in *E. coli* cells and purified from the cytoplasm using Ni-NTA resin and size-exclusion chromatography (SEC) (Fig. 1a). SDS–PAGE analysis and the SEC chromatogram showed that LinkCFQ was in a soluble monomeric form after the final purification (Fig. 1b–d). The apparent molecular weights (MWs) of $^{31–133}$TSG6 and LinkCFQ in solution as determined via multiangle light scattering (MALS) were 12.2 and 12.5 kDa, respectively, which were almost the same as the expected values (Fig. 1e). MW was further analyzed via matrix-assisted laser desorption/ionization–time of flight mass spectrophotometry (Supplementary Fig. 1; m/z: $[M + H]^+$ calculated for $^{31–133}$TSG6: 11551.2, determined: 11548.1; calculated for LinkCFQ: 12544.8, determined: 12540.5). The circular dichroism (CD) spectra of the purified protein were obtained to verify the secondary structure of LinkCFQ (Fig. 2a). The negative peaks observed at 222 nm indicated the presence of an α-helical structure[34]. In addition, the one-dimensional ^{1}H NMR spectra of the native proteins were consistent with those of a previous report[35] (Supplementary Fig. 2). High-field shifted methyl protons (at approximately −0.5 and −1 ppm), which are a characteristic feature of the presence of a stable hydrophobic core, were confirmed. These peaks did not appear in the spectra of the denatured LinkCFQ and $^{31–133}$TSG6. These results imply the proper folding of LinkCFQ. Subsequently, using sigmoidal curve fitting of the negative peak at 222 nm of CD spectra over the temperature range of 25 °C–95 °C, melting temperature (T_m) was determined to be 50.1 °C ± 1.0 °C. As an alternative method, T_m was also measured via differential scanning calorimetry (DSC), resulting in a T_m value of 50.5 °C ± 0.5 °C (Fig. 2b). These results suggest that LinkCFQ is stable at human physiological temperatures. Finally, we analyzed the binding affinity between the purified LinkCFQ and HA via isothermal titration calorimetry (ITC). Here, because the heat change was small and sample volume was limited, the measurement was performed under a condition of *c*-value > 1000[36]. The shape of the binding curve (Fig. 2c) demonstrated that LinkCFQ was bound to high-MW HA (MW: 900,000) with high affinity[36]. In addition, there was no significant difference between $^{31–133}$TSG6 and LinkCFQ regarding the thermodynamic parameters obtained from the ITC analysis summarized in Table 1 and Supplementary Table 1. An additional ITC analysis using HA octasacchaide (HA8) in morpholinoethanesulfonic acid sodium salt (MES) buffer at pH 6.0 demonstrated that although our thermodynamic parameters ($\Delta H = -6.3$ kcal/mol, Supplementary Fig. 3 and Supplementary Table 2) were different from those of a previous study reported by Higman et al. ($\Delta H = -8.0$ kcal/mol)[37], the HA-binding property of LinkCFQ was evident and there was no significant difference in thermodynamic parameters between LinkCFQ and $^{31–133}$TSG6. These results indicated that the MTG-reactive tag was successfully introduced without impairing the activity of $^{31–133}$TSG6.

MTG reactivity of LinkCFQ in the formation of Link–protein conjugates depends on the pI values of the substrates. To evaluate the MTG reactivity of the purified LinkCFQ, various

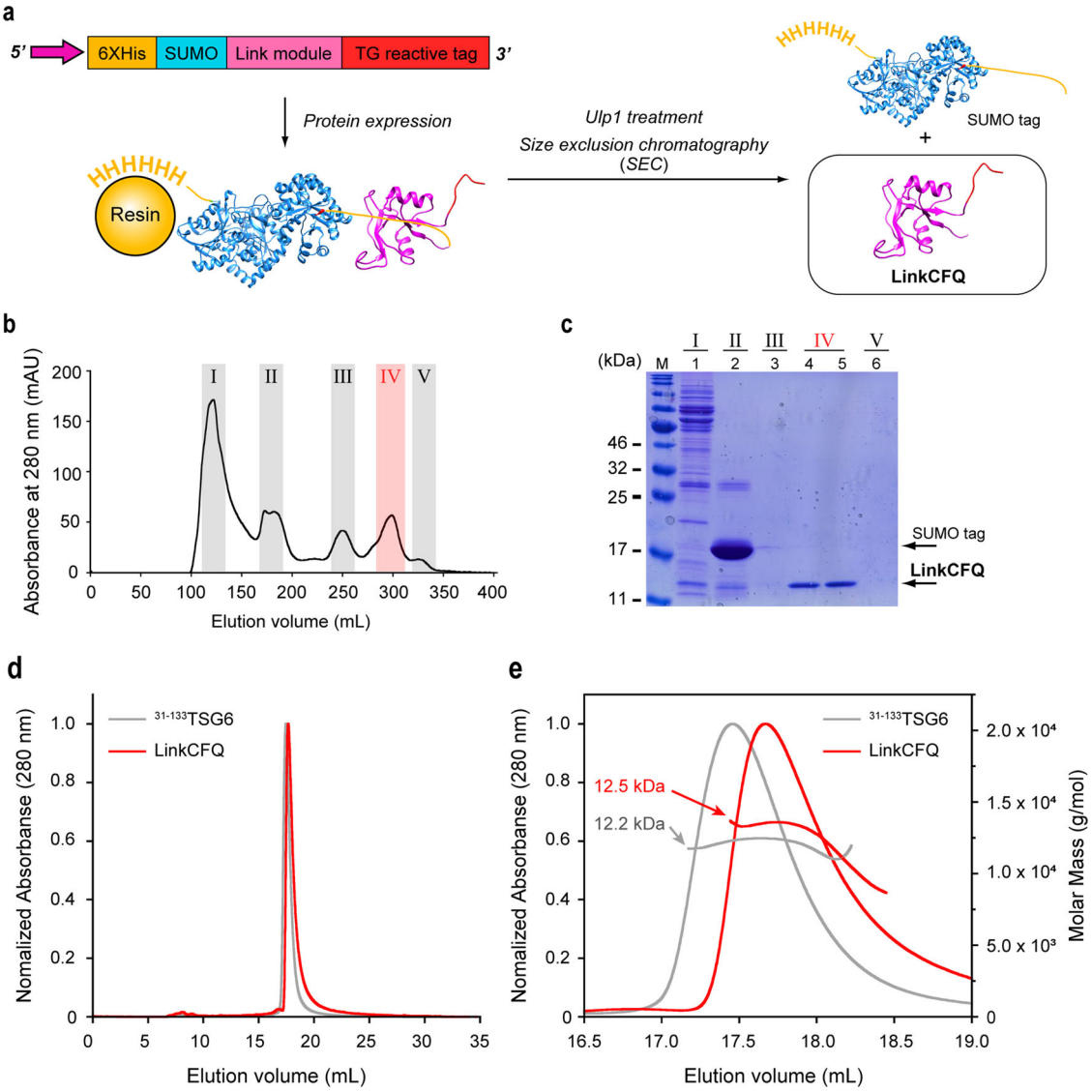

Fig. 1 Expression and purification of LinkCFQ. a Schematic illustration: a 6HisSUMO-tag was introduced at the N-terminal of LinkCFQ, and LinkCFQ was expressed using BL21(DE3). Following enzymatic digestion with Ulp1, LinkCFQ was purified via size-exclusion chromatography (SEC). **b** SEC chromatograph. **c** Sodium dodecyl sulfate-polyacrylamide gel electrophoresis analysis of the fractions, separated via SEC (lanes 4 and 5 are different samples in fraction IV). All samples are reduced. **d**, **e** SEC chromatogram and molecular weight plots of purified proteins determined via multiangle light scattering.

proteins with different pI values (4.78–8.34) were conjugated with LinkCFQ (Table 2 and Fig. 3). At pH values 8.0 and 9.0, LinkCFQ reacted with all proteins but casein and fibrinogen, regardless of their pI values. In general, good substrates for transglutaminase reactions, such as casein[38] and fibrinogen[39], showed an excellent reactivity (>90%). This result indicated that MTG reactivity was successfully introduced into LinkCFQ via MTG-reactive tag functionalization.

To evaluate the MTG reactivity of LinkCFQ with ECM components, we selected fish gelatin as a substrate because of its good handling, which is attributable to its low sol–gel transition temperature (ca. 4–5 °C; Supplementary Fig. 5)[40]. Gelatin is a heterogeneous mixture of peptides derived from collagen, which is the most abundant ECM protein. The MTG-catalyzed conjugation reaction reached a plateau at ~4 h. Strong reactivity was observed at pH values 8.0 and 9.0 of >80% (Fig. 4b, c and Supplementary Fig. 6). This reactivity was not affected by salt concentration (Supplementary Fig. 7). A further SEC–MALS analysis revealed that although HA mixed with MTG-crosslinked gelatin and LinkCFQ did not exhibit significant changes in the chromatogram and MW, the peak of HA mixed with gelatin–Link appeared within a faster retention time than did HA and the MW of HA mixed with gelatin–Link increased substantially from 2.35 × 10^6 to 8.32 × 10^6. In addition, the light scattering (LS) and ultraviolet-visible (UV) overlapping chromatograms also suggested the colocation of HA and gelatin–Link (Supplementary Fig. 8 and Supplementary Table 3). These results imply that even after gelatin conjugation, LinkCFQ retained HA-binding properties. Then, for the first time, an ECM-inspired hydrogel was fabricated with LinkCFQ using HA and a collagen derivative, gelatin, using the natural HA/Link module interaction and TG-catalyzed isopeptide bond formation (Fig. 5a). Regarding physical appearance of the hydrogel, although a whitish gel was obtained without LinkCFQ, the ECM-inspired hydrogel fabricated using LinkCFQ was transparent (Fig. 5b). This suggested that gelatin and HA were homogeneously distributed inside the hydrogel because of the LinkCFQ-mediated crosslinking between gelatin and HA. Consequently, the physical strength of the hydrogel was

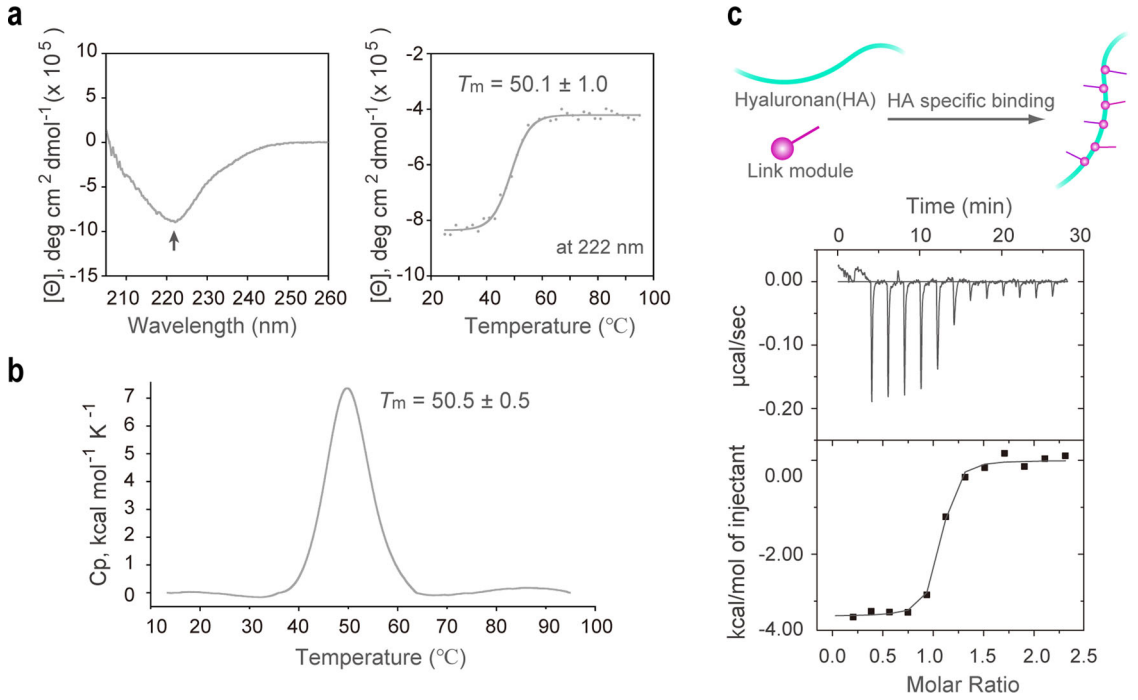

Fig. 2 Physicochemical properties of the purified LinkCFQ. a Representative curve of the circular dichroism spectra of LinkCFQ. A negative peak at 222 nm (arrow) indicated the presence of an α-helix structure. T_m was determined to be 50.1 °C ± 1.0 °C based on sigmoidal curve fitting using Eq. 1. The T_m value was expressed as means ± standard deviations (SDs). **b** Representative curve of the thermal stability of LinkCFQ measured via differential scanning calorimetry. T_m was determined to be 50.5 °C ± 0.5 °C (expressed as means ± SDs). **c** Representative curve of calorimetric titration of LinkCFQ (15 μM) with HA (octasaccharide unit concentration, 150 μM). Data were fitted to the one-site binding model.

Table 1 Thermodynamic parameters of interaction between LinkCFQ and HA.

Protein	HA	pH	Buffer	ΔH[a] (kcal/mol)
$^{31-133}$TSG6	MW: 900,000	7.4	5 mM MES	−5.30 ± 0.31[b]
LinkCFQ	MW: 900,000	7.4	5 mM MES	−5.19 ± 0.11[b]

ΔH change in enthalpy, *MES* morpholinoethanesulfonic acid sodium salt.
[a]Because the heat change was small and sample volume was limited, the measurements were performed under a condition of *c*-value >1000. Before fitting, the heats of HA dilutions in the buffer were subtracted.
[b]Considering inherent inaccuracy in the concentration of HA, based on the published study by Blundell et al for Link_TSG6[62], the ITC titrations were fitted by assuming a 1:1 stoichiometry for the interaction of HA10 (a decasaccharide) with $^{31-133}$TSG-6 and LinkCFQ. The parameters obtained from raw experimental conditions were shown in Supplementary Table 1.
All data represent the means of three independent isothermal titration calorimetry experiments (±standard deviations).

increased through the LinkCFQ-mediated crosslinking (Fig. 5c). The storage modulus (G') of the ECM-inspired hydrogel was ca. 200 Pa, which was similar to that of HA-rich soft tissues such as the brain tissue[41].

Finally, we evaluated the biocompatibility of the ECM-inspired hydrogel in vitro and in vivo. Because intraperitoneal administration (i.p.) was one of the expected applications (i.e., HA-based anti-adhesion material such as Seprafilm®), mesothelial cells (MeT5A), which possibly contact with i.p.-administered material and play a crucial role in maintaining homeostasis of the abdominal cavity[42], were used as the model cells. Of note, we used a cell line in the first step to evaluate the basic biocompatibility of the hydrogel, although evaluating it using primary cells in the future is recommended. Met5A were cultured on the ECM-inspired hydrogel (Fig. 6a). After 2 days of culture, which was the minimal time point at which we could confirm the attachment and growth of cells, on the ECM-inspired hydrogel, live cells (green) were identified using confocal microscopy; they attached to the hydrogel surface and grew (Fig. 6b). In addition, the ECM-inspired hydrogel was subcutaneously administered into mice (Fig. 6c). To determine the effect of the materials on acute immune response, we evaluated the outcomes 3 days after administration. The ECM-inspired hydrogel was mostly degraded, whereas the residues of a commercially available hydrogel fibrin glue were observed. Hematoxylin−eosin (H&E) staining of the surrounding tissues and hydrogel residues showed that a few lymphocytes were present at the administration site, which was similar to that noted in the control group that did not receive hydrogel (Fig. 6d). In addition, compared with that noted after the administration of hydrogel without LinkCFQ, the edema induced by the ECM-inspired hydrogel appeared to be mild. Overall, the ECM-inspired hydrogel exhibited biodegradability and biocompatibility.

Discussion

The aspect of the ECM-inspired hydrogel for future applications such as mechanical properties and biofunction has not been studied yet. The present study focused on the design of the ECM-inspired material, including Link module/HA interaction as a building block, as a first step. The Link module is observed abundantly and seems to be of great importance in the natural ECM structure. Hence, the present material design is useful and may be applied in medical settings.

In the present study, we designed LinkCFQ as a genetically engineered protein linker. During the development, we examined the process of using the full Link_TSG6 domain itself to improve production yield. In previous reports, Link_TSG6 was expressed in an insoluble form in *E. coli*; thus, the refolding process was necessary to activate the protein[35,43].Thus, we introduced a SUMO-tag at the N terminus of the protein and then used a

Table 2 Characteristics of model proteins used for evaluating the effect of pI value on the MTG-catalyzed conjugation reaction.

Protein name	pI	MW	Lys	Gln	Total (amino acid)
EGF	4.78	6222	2	1	53
Insulin	5.22	11981	2	7	110
β-casein	5.28	44672	25	22	430
HSA	5.60	66462	59	20	583
Fibrinogen	6.36	159632	100	67	1434
Transferrin	6.70	75195	58	17	679
Myoglobin	7.36	16951	19	6	153
Lactoferrin	8.34	75982	46	26	691

pI value was calculated via Expasy using the ProtParam tool (https://web.expasy.org/protparam/).

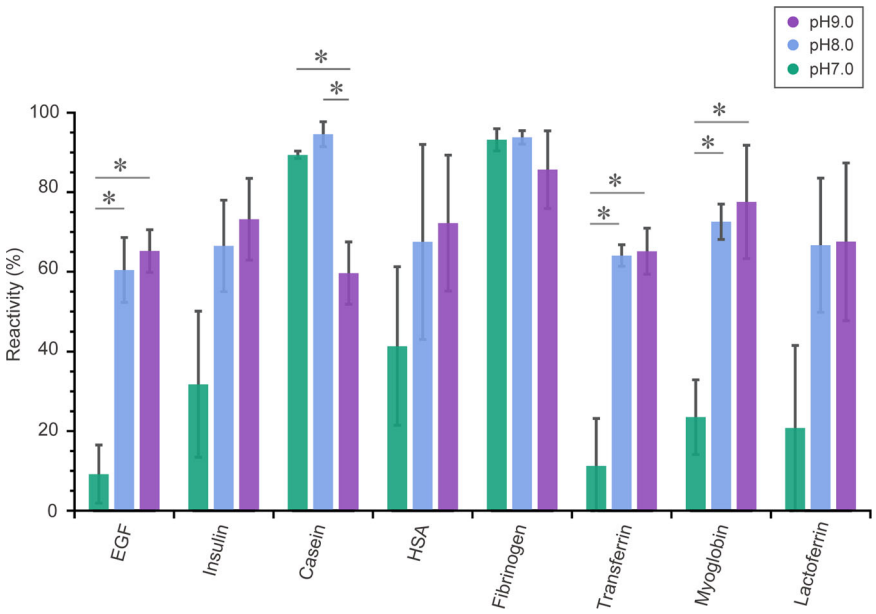

Fig. 3 MTG-catalyzed conjugation of LinkCFQ to substrate proteins with pI values of 4.78–8.34 at different pH values (pH 7, 8, and 9). The reaction was evaluated via sodium dodecyl sulfate-polyacrylamide gel electrophoresis, followed by staining with Coomassie brilliant blue (Supplementary Fig. 4). Reactivity (%) was defined and calculated using Eq. 3. All error bars represent standard deviations. *$P < 0.05$.

vector system for low temperature expression and chaperone coexpression. Consequently, the protein was expressed in a soluble form in *E. coli* and the resulting purification yield was up to 2 mg/L at the culture scale. This allowed the culture system to be easily scaled up, which was required to obtain a sufficient amount of Link_TSG6 to fabricate ECM-inspired hydrogels.

Regarding its physicochemical properties, LinkCFQ successfully retained the characteristics of $^{31-133}$TSG6 (Fig. 2). In particular, regarding the HA-binding property, LinkCFQ was bound to every 6.6 ± 0.5 oligosaccharides along the HA chain (Supplementary Table 1). This shows the feasibility of designing a natural proteoglycan-like structure in the hydrogel with up to ca. 720 LinkCFQ moieties strung together in a single 900-kDa HA comprising 4750 oligosaccharides. In addition, the HA-binding affinity of LinkCFQ ($K_a = 17.4 \times 10^6\ M^{-1}$ under low-salt conditions) was relatively higher than that of HA-binding peptide mimetics[44] and other lectins[45,46] ($K_a < 1.0 \times 10^6\ M^{-1}$), although it was weaker than that of antibodies[47] (K_a of the order of $1.0 \times 10^8\ M^{-1}$). We evaluated the binding of LinkCFQ to HA8 under physiological conditions using phosphate buffer saline (PBS; –) at pH 7.4 (Supplementary Fig. 9 and Supplementary Table 4). Because the interaction between the Link module and HA is in part mediated by ionic interactions[48], the binding of LinkCFQ to HA became weaker ($0.09 \times 10^6\ M^{-1}$, here K_a is an estimate since the value was obtained by fitting near the experimental limit with *c-value* ranging from 1 to 3 in all experiments). It was also confirmed that LinkCFQ maintained its HA-binding property under physiological salt conditions. In addition, we confirmed the difference in thermodynamic parameters between $^{31-133}$TSG6 and Link_TSG6 (Supplementary Fig. 3 and Supplementary Table 2). Of note, this might have resulted from differences in the experimental conditions such as the bound water content of HA, sequence of amino acids, etc. Because there are several possible reasons for this difference, we will investigate it in greater details in a future study.

In the design of ECM-mimetic hydrogels, materials have been developed that mimic the crosslinked structure of the ECM in nature. Chemical crosslinking observed in the integration of collagen fibrils and proteoglycan is represented by Schiff bases[27], isopeptide bonds[29], and O-glycoside bonds[49]. Various materials have been developed using these chemical crosslinkers to achieve ECM-mimetic properties[50,51]. Another type of crosslinking in the natural ECM is physical crosslinking, represented by hydrogen bonds, van der Waals forces, and ionic bonds, which is the primary mechanism underlying the binding of the Link module to HA in proteoglycans[17]. The interaction between HA and Link module is highly selective; thus, no nonspecific reaction occurs, which can prevent toxicities and the risk of frequently used

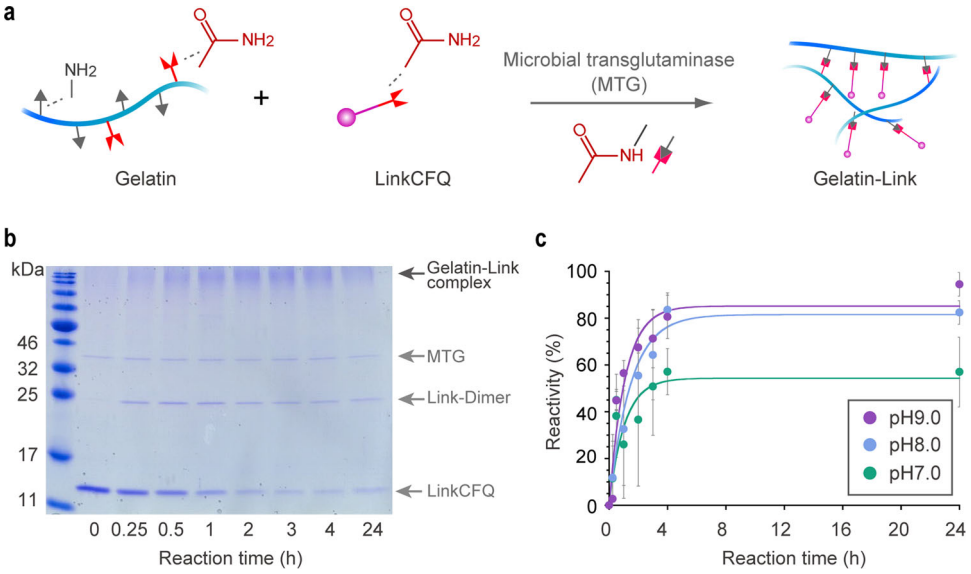

Fig. 4 MTG-catalyzed conjugation reaction between LinkCFQ and gelatin. a Purified LinkCFQ was crosslinked with fish gelatin at different pH values (pH 7, 8, and 9) at 4 °C for 0–24 h. **b** Representative images of sodium dodecyl sulfate–polyacrylamide gel electrophoresis analysis of the reaction mixture at pH 8.0. Other images, at pH 7–9, are presented in Supplementary Fig. 6. **c** Reactivity (%) was defined and calculated using Eq. 3. The time course of experimental enzyme-catalyzed reactivity (%) was fitted using Eq. 4[64]. Glutamine and lysine residues are illustrated using red and gray graphics, respectively. All error bars represent standard deviations.

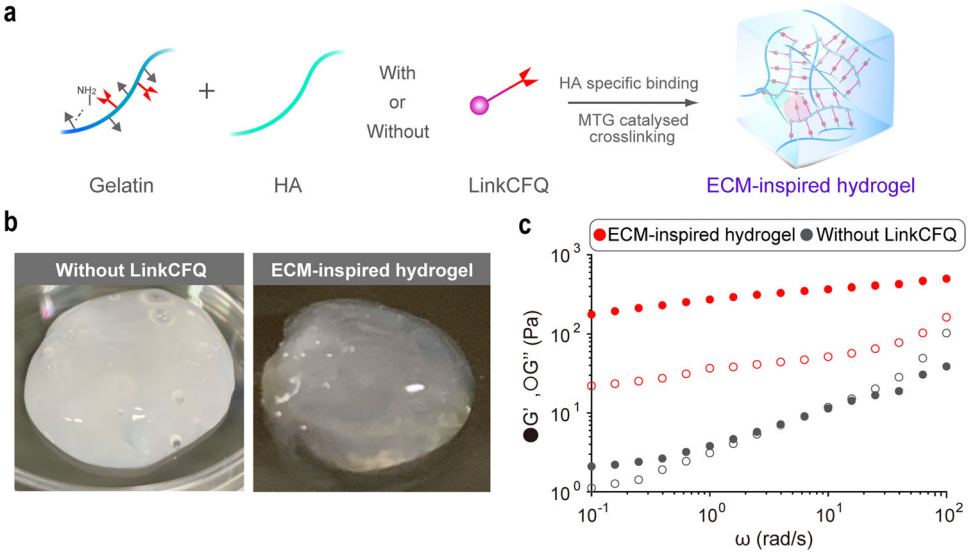

Fig. 5 Fabrication of ECM-inspired hydrogel with LinkCFQ. a Schematic illustration of ECM-inspired hydrogel formation. **b** Representative image of the fabricated ECM-inspired hydrogel. **c** Dynamic viscoelastic property of the fabricated ECM-inspired hydrogel. Glutamine and lysine residues are illustrated using red and gray graphics, respectively.

chemical crosslinking. In addition, this physical crosslinking is reversible at different pH values[52], thereby playing important roles in the ECM remodeling. However, owing to the interdisciplinary nature of material engineering and protein engineering, to the best of our knowledge, although peptide mimetics have partially attained these crosslinking characteristics[44], no studies have completely reproduced the interaction between HA and the Link module. The present study, in which a fusion protein with the full Link_TSG6 structure was designed, may contribute significantly to the design and development of such materials.

Expanding the range of functionalization is important to broaden the scope of the future application of LinkCFQ. Therefore, various functional LinkCFQ modalities were prepared by conjugation with ECM components, growth factors, and several proteins via MTG-catalyzed reaction (Fig. 3). Considering the pI values of LinkCFQ (9.5) and MTG[53] (8.9), the rate-limiting step of this reaction is mainly the complex formation between substrates and enzymes, which resulted in excellent reactivity at approximately pH 8.0. However, there are some exceptions for proteins with high reactivity, such as casein and fibrinogen, which might be attributed to the differences in protein structure, number of functional groups, etc. Thus, we will investigate this further in our future study.

As an example of the applications of LinkCFQ modalities, a green fluorescent protein (GFP)–conjugated modality (Link-GFP)

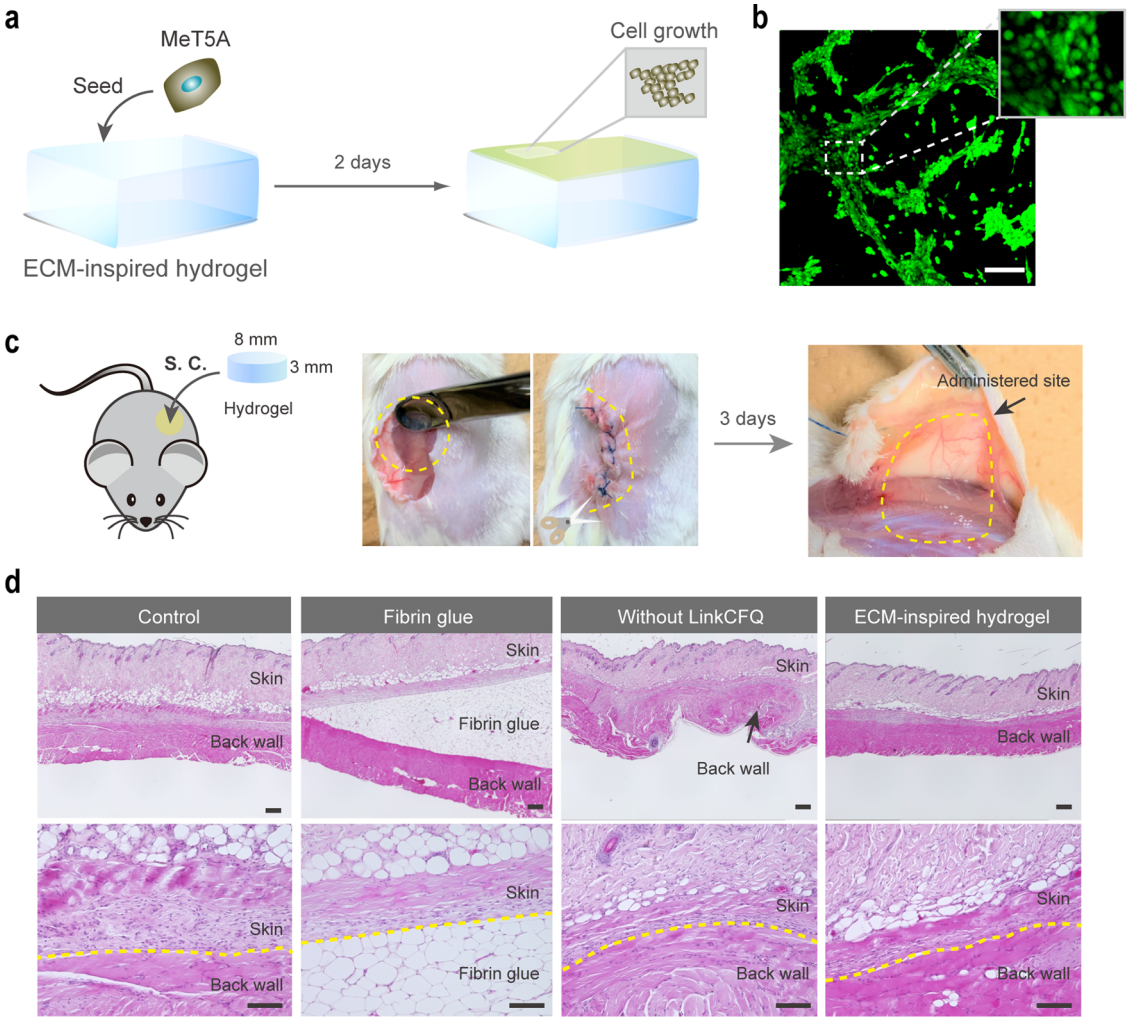

Fig. 6 Evaluation of the biocompatibility of the fabricated ECM-inspired hydrogel. a Schematic illustration of the effect of the ECM-inspired hydrogel on cultured cells. **b** Confocal laser microscopic observation of cells cultured on the fabricated ECM-inspired hydrogel. Live cells were stained with Calcein acetoxymethyl ester (Calcein-AM; green). Scale bar, 100 μm ($N = 2$). **c** Schematic illustration of the subcutaneous administration of ECM-inspired hydrogel into mice. The administration site was evaluated 3 days after the administration. **d** Hematoxylin−eosin staining of the skin tissue of mice administered with fibrin glue, hydrogel without LinkCFQ, and ECM-inspired hydrogel. Mice that received no material were used as the control. Scale bar: 200 μm (upper image) and 100 μm (lower image; $N = 2$).

was prepared to functionalize the ECM-inspired hydrogel, which succeeded in binding the hydrogel more efficiently than the control group, without the Link module (Supplementary Fig. 10 and Supplementary Fig. 11). TSG-6 comprises a Link module and a CUB domain. TSG-6 binds HA via the Link module, whereas the CUB domains of two TSG-6s associate and naturally work as crosslinkers of HA[19]. The key to the present success may lie in the design of LinkCFQ where the MTG-reactive tag was introduced, i.e., the C-terminal of $^{31-133}$TSG6 at the site of the CUB domain. Therefore, various conjugated components are expected to exert their function without the loss of $^{31-133}$TSG6 activity.

Considering the application of our technique in the field of tissue engineering and regenerative medicine, biocompatibility and the applicable dose of the protein are of great interest. In this study, the dose of ca. 2.7 mg/kg (225 nmol/kg) protein was administered subcutaneously into mice with the hydrogel and showed biocompatibility (Fig. 6c, d). Previously, fusion proteins including Link_TSG6 were administered intraocularly, intratumorally, and intravenously at dose ranging from 6.2 to 35 nmol/kg[54–58] (Supplementary Table 5). In comparison, our dose was relatively high, but did not induce severe inflammation. This suggests that when the protein was administered in complex with HA, high-dose administration of the protein was possible. Our study may provide important insights into the design of Link module-based biomaterials for future applications.

Recently, HA-rich extracellular matrices such as those observed in cancer microenvironments, ocular tissues, skin, and cartilage regions have attracted considerable attention in the field of drug discovery and development. Previously, Link_TSG6-based fusion proteins were developed for the treatment of cancer[55] and retinal diseases[56]. Both of the aforementioned studies suggested that the HA-binding property of Link_TSG6 prolonged drug retention time within HA-rich environments and improved therapeutic efficacy. Furthermore, LinkCFQ may enable the conjugation of small- and medium-sized molecules and antibody drugs, which may lead to the development of various effective therapies.

In the field of tissue engineering, the top-down approach has been advanced after the emergence of decellularized methods[9]. Although the bottom-up approach has been examined in several studies on elemental biomacromolecules, owing to the difficulty of isolation, each ECM element, particularly proteins, is not yet used as a building block. The Link module is one of these missing

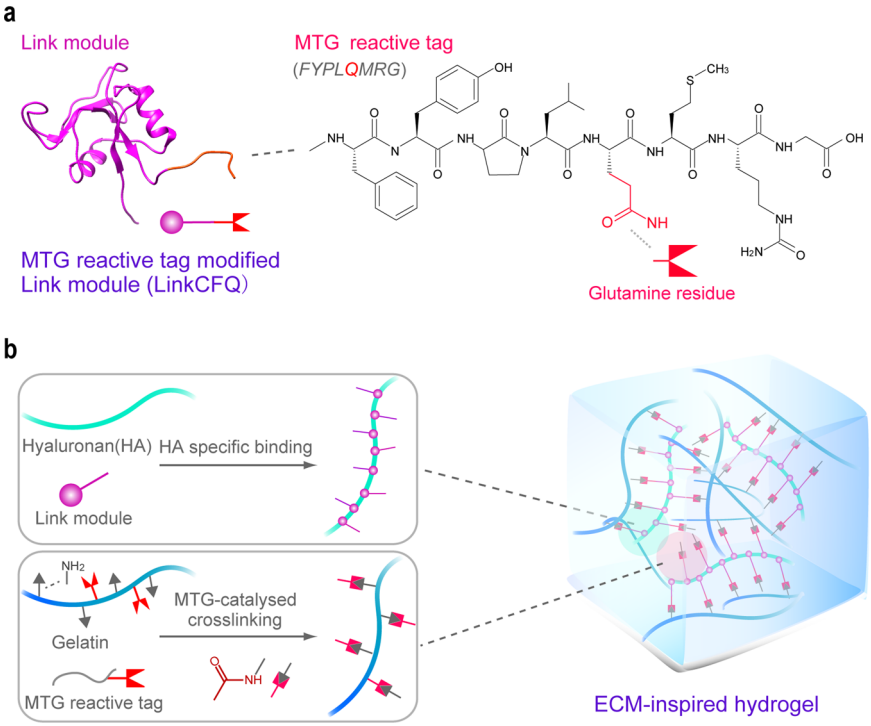

Fig. 7 Schematic illustration of LinkCFQ and ECM-inspired hydrogel. a Structure of the genetically engineered Link module (LinkCFQ) was predicted via the MODELLER software using Link_TSG6 (PDB ID: 1O7c)[65] as the template. LinkCFQ was designed with a C-terminal extension using the MTG-reactive tag (FYPLQMRG) in the Link module. **b** ECM-inspired hydrogel fabricated with LinkCFQ using HA and gelatin through the incorporation of the natural HA/Link module interaction and formation of the MTG-catalyzed isopeptide bond. Glutamine and lysine residues are illustrated using red and gray graphics, respectively.

ECM elements. Thus, the present study has profound significance in the field of tissue engineering and regenerative medicine.

Recently, the bioprinting field has developed tremendously[59,60]; Our strategy can be combined further with bioinks that reproduce the properties of the native ECM for advanced applications in tissue engineering. The strategy used in the present study for the development of the ECM-inspired hydrogel provides a reference for future strategies for bioink design.

Conclusion

We designed and successfully purified a genetically engineered Link module (LinkCFQ) with HA-specific binding property and TG reactivity. Although the physicochemical properties of the Link module were preserved, LinkCFQ demonstrated excellent MTG reactivity with various proteins to form Link–protein conjugates. To the best of our knowledge, this study is the first to fabricate an ECM-inspired hydrogel with LinkCFQ. The biocompatibility and degradability of the ECM-inspired hydrogel were confirmed through cell culture experiments in vitro and animal experiments in vivo. The fabricated ECM-inspired hydrogel with LinkCFQ seems promising for biomedical applications; thus, our findings provide insights into the design of bioinspired materials for tissue engineering and regenerative medicine.

Methods

Materials. HA (MW, ca. 900,000 Da) was kindly gifted by Denka Co. (Tokyo, Japan), microbial transglutaminase (MTG) was kindly gifted by Ajinomoto Co. Inc. (Tokyo, Japan), and fish gelatin was kindly gifted by Niita Gelatin Co. (Osaka, Japan; MW, ca. 60 kDa). Dialysis membrane (Spectra/Por, MW cutoff 6–8 kDa) was purchased from Spectrum Laboratories Inc. (Nevada, USA). Human recombinant insulin, casein, fibrinogen, human serum albumin, transferrin, lysozyme, myoglobin, and lactoferrin were purchased from FUJIFILM Wako Pure Chemical Co. (Osaka, Japan).

Protein design, expression, and purification. We designed the genetically engineered Link module ($^{31-133}$TSG6-CFQ, LinkCFQ) with a C-terminal extension of a Gln-donor substrate peptide tag (FYPLQMRG)[32] to the Link module (Fig. 7a), amino acids 31–133 (UniProtKB: P98066) in the preprotein, from human TSG-6 ($^{31-133}$TSG6) to fabricate the ECM-inspired hydrogel (Fig. 7b). The cDNA of LinkCFQ was purchased from Integrated DNA Technologies, Inc. (Iowa, USA) and subcloned into a pCold I vector (TAKARA Bio Inc., Shiga, Japan) with an N-terminal six histidine-SUMO-tag (pCold-6HisSUMO-LinkCFQ). pCold-6HisSUMO-LinkCFQ and the molecular chaperone plasmid pG-TF2 (TAKARA Bio Inc., Shiga, Japan) was coexpressed using the BL21(DE3) expression system with Luria–Bertani medium. Briefly, BL21(DE3) was cultured at 37 °C until the O.D. reached 0.6; then, protein expression was induced using isopropyl β-D-1-thiogalactopyranoside (final concentration, 500 μM), followed by incubation for 20–24 h at 15 °C. Pellets of *E. coli* cells were resuspended in 20 mM Tris–HCl buffer (pH 8.0) containing 500 mM NaCl and 5 mM imidazole. The cells were disrupted via sonication and centrifuged at 40,000 *g* for 30 min. The supernatants were loaded to a volume of 1 mL in a column of Ni-NTA resin (QIAGEN, Hilden, Germany). The column was washed with 5 mL of a buffer containing 500 mM NaCl, 20 mM Tris–HCl pH 8.0, and 5–20 mM imidazole and then eluted with 5 mL of another buffer containing 500 mM NaCl, 20 mM Tris–HCl pH 8.0, and 50–500 mM imidazole. To remove the 6HisSUMO-tag, the eluted 6HisSUMO-LinkCFQ was incubated with the Ulp1 enzyme, which cleaved the 6HisSUMO-tag from the protein, in a dialysis membrane with 50 mM Tris–HCl, 200 mM NaCl, and 100 mM arginine at 4 °C for over 12 h. LinkCFQ was then purified via SEC using the HiLoad 26/60 Superdex 75 pg column (GE Healthcare, IL, USA). The purity of all proteins was analyzed via sodium dodecyl sulfate–polyacrylamide gel electrophoresis (SDS–PAGE), followed by staining with Coomassie brilliant blue. We produced recombinant $^{31-133}$TSG6 using the same method as that used for LinkCFQ. The amino acid sequence alignment is shown in Supplementary Fig. 12. Our $^{31-133}$TSG6 was 6 amino acids (SLERAA) longer at the N terminus than the Link_TSG6 (36–133) used by Higman et al.[37].

Circular dichroism. To confirm that the introduction of the MTG-reactive tag did not disrupt the secondary structure of the Link module, its CD spectra was measured at 25 °C in 5 mM MES buffer at pH 7.4 using quartz cells with a 1-mm path length (J-820; JASCO, Tokyo, Japan). The instrument parameters were as follows: bandwidth, 1 nm; time constant, 1 s; scan rate, 20 nm/min; and scan number, 5. The protein sample was equilibrated in 5 mM MES buffer at pH 7.4 through dialysis (>100-fold volume) and concentrated to 30 μM. As described before[61], Protein concentrations were determined by measuring absorbance at 280 nm using

a NanoDrop spectrophotometer (Thermo Fisher Scientific, MA, USA) with extinction coefficients of $^{31-133}$TSG6 (23170 M^{-1} cm^{-1}) and LinkCFQ (24660 M^{-1} cm^{-1}), as calculated using ProtParam (https://web.expasy.org/protparam/). The spectrum for buffer alone was subtracted from that for LinkCFQ. To determine the transition temperature of the secondary structure conversion, the CD signal was monitored at 222 nm over a temperature range of 25 °C–95 °C at a rate of 1 °C /min. The CD values were analyzed using the Spectra Manager software Version 1.55.00 (JASCO, Tokyo, Japan) and converted to mean residue ellipticity. T_m was determined by sigmoidal curve fitting via KaleidaGraph (Hulinks, Tokyo, Japan) using Eq. 1.

$$y(\Theta) = a + \frac{b}{1 + \exp(-\frac{x - Tm}{c})} \quad (1)$$

Differential scanning calorimetry. The thermal stability of LinkCFQ was measured using the automated PEAQ-DSC microcalorimeter (MicroCal PEAQ-DSC; GE Healthcare, Illinois, USA). Before use, the protein sample was equilibrated in 5 mM MES buffer at pH 7.4 via dialysis (>100-fold volume) and concentrated to 60 μM. The sample was scanned over a temperature range of 10 °C–95 °C at a rate of 1 °C /min. Data were analyzed using the Origin software (OriginLab, MA, USA).

Isothermal titration calorimetry. Thermodynamic parameters of the interaction between LinkCFQ and high-MW HA (MW: 900,000) were determined using the iTC200 (GE Healthcare, IL, USA). Before use, HA (MW: 900,000) was desalinated in pure water via dialysis (>100-fold volume) and then lyophilized. The protein sample was equilibrated in 5 mM MES buffer at pH 7.4 via dialysis (>100-fold volume), and HA (MW: 900,000) was prepared in the same buffer. First, we prepared a 2 mg/mL stock solution. HA (ca. 10 mg; MW: 900,000) was weighed and dissolved in ca. 5 mL of the buffer. Then, the stock solution was diluted to the working concentration. In our experimental design, 15 μM protein was placed in the cell and 0.277 mg/ml HA (MW: 900,000), which corresponds to 150 μM HA8 unit concentration, was taken into the ITC syringe. The abovementioned concentration of HA was calculated based on an assumption that HA comprises repeated units of the polymeric disaccharides D-glucuronic acid and *N*-acetyl-D-glucosamine (MW: 379). Aliquots of 0.5 μl × 1 and 3 μl × 12 were injected into the reaction cell at 120-s intervals with a stirring speed of 750 rpm and a temperature of 25 °C.

The thermodynamic parameters of the interaction between LinkCFQ and HA8 (H1148, TCI, Tokyo, Japan) were determined using a VP-ITC instrument (GE Healthcare, IL, USA). Before use, the protein sample was equilibrated in 5 mM MES buffer at pH 6.0 or PBS (–) at pH 7.4 via dialysis (>100-fold volume). HA8 (MW: 1535) was prepared in the same buffer. First, we prepared a 2 mg/mL stock solution via the reconstitution of 1 mg HA8 with 500 μl of the ITC buffer. Subsequently, the stock solution was diluted to the working concentration. In our experimental design, 15 μM protein was placed in the cell and 150 μM (0.230 mg/ml) HA8 was taken into the ITC syringe. Aliquots of 5 μl × 1 and 10 μl × 24 were injected into the reaction cell at 120-s intervals with a stirring speed of 307 rpm and a temperature of 25 °C. The measurement was performed thrice. Binding isotherms were fitted to a one-site binding model using ORIGIN 7.0 after subtracting the heats generated by HA dilutions in the buffer in a separate experiment. We determined the binding number of oligosaccharide HA per LinkCFQ using the concentration when the binding ratio was 1.00 ± 0.05 by fitting. In addition, considering inherent inaccuracy in the concentration of HA, based on the published study by Blundell et al. for Link_TSG6, the ITC titrations were fitted by assuming a 1:1 stoichiometry for the interaction of HA10 with LinkCFQ[62]. As for HA8, a 1:1 stoichiometry was assumed for the interaction of HA8 with LinkCFQ as well[37]. Using the same condition as that used for LinkCFQ, the thermodynamic parameters of $^{31-133}$TSG6 were also determined, for comparison. To evaluate the quality of the data, the *c-value* was calculated using Eq. 2. Here in the range of *c*-values from ca. 1 to 1000, K_a values were obtained following the definition of Wiseman et al.[63].

$$C - \text{value} = \text{Binding ratio} \times \text{Concentration of protein} \times K_a \quad (2)$$

MTG-catalyzed conjugation between LinkCFQ and various proteins. The purified LinkCFQ (5 μM) was crosslinked with various proteins (25 μM) with pI values ranging from 4.78 to 8.34. The reaction was performed using 0.1 U/mL MTG in 50 mM Tris–HCl buffer containing 100 mM NaCl with different pH values (pH 7, 8, or 9) at 4 °C for 24 h. The reaction was then stopped by the addition of SDS–PAGE sample buffer containing an excess amount of β-mercaptoethanol, followed by boiling for 5 min. The reaction mixture was then evaluated via SDS–PAGE, followed by staining with Coomassie brilliant blue. The reaction efficacy was analyzed using the ImageJ software (the National Institutes of Health [NIH], MD, USA) using the LinkCFQ band at ~12 kDa. The reactivity was defined and calculated using Eq. 3.

$$\text{Reactivity}\,(\%) = \left(1 - \frac{\text{LinkCFQ band Intensity (each time)}}{\text{LinkCFQ band Intensity (0 h)}}\right) \times 100 \quad (3)$$

MTG-catalyzed conjugation between LinkCFQ and gelatin. The purified LinkCFQ (5 μM) was crosslinked with fish gelatin (0.01 wt%, containing ca. 25 μM lysine residues) using 0.1 U/mL MTG in 50 mM Tris–HCl containing 100 mM NaCl with different pH values (pH 7, 8, and 9) at 4 °C for 0–24 h. The reaction was stopped by the addition of SDS–PAGE sample buffer containing an excess amount of β-mercaptoethanol, followed by boiling for 5 min. The reaction mixture was evaluated via SDS–PAGE, followed by staining with Coomassie brilliant blue. The reaction efficacy was analyzed using the ImageJ software (NIH, MD, USA) using the LinkCFQ band at approximately 12 kDa. Time courses of experimental enzyme-catalyzed reactivity (%) were fitted by the product inhibition/substrate depletion equation[64] via KaleidaGraph (Hulinks, Tokyo, Japan) using Eq. 4.

$$\text{Reactivity}\,(\%) = \frac{\nu_0}{\eta} \times (1 - e^{-\eta t}) \quad (4)$$

where ν_0 represents the initial enzyme cycling velocity and η represents the reduction in cycling velocity that caused nonlinearity in the time course.

Fabrication of ECM-inspired hydrogel and rheological analysis. The ECM-inspired hydrogel was fabricated via MTG-catalyzed crosslinking with 1.25 wt% HA, 1.25 wt% gelatin, 1 U/mL MTG, and 30 μM LinkCFQ in Tris–HCl buffer (50 mM Tris–HCl and 100 mM NaCl; pH 8.0) inside a silicon mold at 4 °C for 24 h. The dynamic oscillatory frequency experiment was performed using a rheometer (MCR301; Anton Paar, Graz, Austria) with parallel-plate geometry (PP25; diameter = 25 mm, gap = 1.0 mm).

Hydrogel functionalization of Link–protein conjugates. LinkCFQ (5 μM) was crosslinked with GFP (25 μM) using 0.1 U/mL MTG in Tris–HCl buffer (50 mM Tris–HCl and 100 mM NaCl; pH 8.0) at 4 °C for 24 h to form Link-GFP. A total volume of 200 μL ECM-inspired hydrogel (1.25 wt% gelatin, 1.25 wt% HA, 30 μM LinkCFQ, and 1 U/mL MTG) in Tris–HCl buffer (50 mM Tris–HCl and 100 mM NaCl; pH 8.0) was placed on a 35-mm glass-bottomed dish (Matsunami Glass Ind., Ltd., Osaka, Japan) at 4 °C for 24 h. A total volume of 500 μL Link-GFP mixture, including 25 μM GFP, 5 μM LinkCFQ, and 0.1 U/mL MTG with 2 mL PBS, was added to the ECM-inspired hydrogel and incubated with constant shaking at 70 rpm for 24 h at room temperature. The hydrogel was washed twice with PBS. The fluorescence images of bound GFP were collected using the iBright FL1000 Imaging System (Thermo Fisher Scientific Inc., MA, USA). The mean fluorescent intensity of the image was quantified using the ImageJ software (NIH, MD, USA).

Evaluation of biocompatibility of ECM-inspired hydrogel. The evaluation of the biocompatibility of the ECM-inspired hydrogel was performed using a human mesothelial cell line (MeT5A [CRL-9444]; American Type Culture Collection, VA, USA) cultured with medium 199 supplemented with 3.3 nM epidermal growth factor, 361 nM hydrocortisone, 870 nM insulin, 1% Penicillin-Streptomycin-Amphotericin, and 10% fetal bovine serum. Using the same steps as described in the previous section, a total volume of 200 μL ECM-inspired hydrogel was placed on a 35-mm glass-bottomed dish. In total, 5×10^4 cells were placed in each dish with 2 mL of medium and incubated at 37 °C under 5% CO_2 for 3 days. The hydrogels were then washed carefully with PBS and stained with 2 μM Calcein-AM for 10 min. The hydrogel was observed via confocal laser microscopy (FV3000; Olympus, Tokyo, Japan) at 495 nm/520 nm (ex/em).

Subcutaneous administration of ECM-inspired hydrogel. The experiments were performed at the Section for Animal Research, Center for Disease Biology and Integrative Medicine, Faculty of Medicine, The University of Tokyo, Japan. The Animal Care Committee of the University of Tokyo approved all procedures in this study before study commencement. ICR mice (sex, male; age, 3 weeks; weight, 20 g) were purchased from CLEA Japan, Inc. (Tokyo, Japan) and housed in groups under a 12-h (6 a.m.−6 p.m.) light–dark cycle.

The polymers were sterilized with ethylene oxide and then dissolved in PBS at 2.5 wt% concentration. LinkCFQ was further purified via ion-exchange chromatography to eliminate endotoxins and sterilized using a 0.22-μm filter. Anesthesia was induced with isoflurane. The ECM-inspired hydrogel (1.25 wt% gelatin, 1.25 wt% HA, 30 μM LinkCFQ, and 1 U/mL MTG) in PBS was fabricated at 4 °C for 24 h in a silicon mold and formed a cylinder-shaped hydrogel (diameter, 8 mm; height, 3 mm). The obtained hydrogel was then administered subcutaneously into the left side of the back of the mice. To compare with a biocompatible hydrogel, some mice were administered with an equal amount of fibrin glue. At 3 days after administration, the mice were euthanized and the presence of residues was evaluated. Residual hydrogels with surrounding tissues were sampled, fixed in 10% formalin, and then processed on slides for H&E staining and histological evaluation via standard techniques. The obtained H&E-stained slides were observed under a microscope (BZ-X9100; Keyence Co, Osaka, Japan).

Statistical analysis. Each experiment was repeated thrice, unless mentioned otherwise. Analysis of variance and then Tukey's post hoc test were performed for data analysis using KaleidaGraph 4.0 J (Hulinks, Tokyo, Japan), unless otherwise specified. Significance was set at $P < 0.05$.

Reporting summary. Further information on research design is available in the Nature Research Reporting Summary linked to this article.

Data availability

The datasets generated and/or analyzed during this study are available from the corresponding author on reasonable request.

Received: 23 November 2021; Accepted: 20 October 2022;
Published online: 30 October 2022

References

1. Zolotovsky, K. et al. Fish-inspired flexible protective material systems with anisotropic bending stiffness. *Commun. Mater.* **2**, 1–10 (2021).
2. Mahdavi, A. et al. A biodegradable and biocompatible gecko-inspired tissue adhesive. *Proc. Natl. Acad. Sci. USA* **105**, 2307–2312 (2008).
3. Bharadwaz, A. & Jayasuriya, A. C. Recent trends in the application of widely used natural and synthetic polymer nanocomposites in bone tissue regeneration. *Mater. Sci. Eng. C* **110**, 110698 (2020).
4. Fu, X. et al. Bioinspired perfluorocarbon-based oxygen carriers with concave shape and deformable shell. *Adv. Mater. Technol.* **2100573**, 1–11 (2021).
5. Sorushanova, A. et al. The collagen suprafamily: from biosynthesis to advanced biomaterial development. *Adv. Mater.* **31**, 1–39 (2019).
6. Amorim, S., Reis, C. A., Reis, R. L. & Pires, R. A. Extracellular matrix mimics using hyaluronan-based biomaterials. *Trends Biotechnol.* **39**, 90–104 (2021).
7. Lee, K. Y. & Mooney, D. J. Alginate: properties and biomedical applications. *Prog. Polym. Sci.* **37**, 106–126 (2012).
8. Oki, Y. et al. Switching of cell proliferation/differentiation in thiol-maleimide clickable microcapsules triggered by in situ conjugation of biomimetic peptides. *Biomacromolecules* **20**, 2350–2359 (2019).
9. Hussey, G. S., Dziki, J. L. & Badylak, S. F. Extracellular matrix-based materials for regenerative medicine. *Nat. Rev. Mater.* **3**, 159–173 (2018).
10. Theocharis, A. D., Skandalis, S. S., Gialeli, C. & Karamanos, N. K. Extracellular matrix structure. *Adv. Drug Deliv. Rev.* **97**, 4–27 (2016).
11. Sani, E. S. et al. Sutureless repair of corneal injuries using naturally derived bioadhesive hydrogels. *Sci. Adv.* **5**, 1–14 (2019).
12. Lou, J., Stowers, R., Nam, S., Xia, Y. & Chaudhuri, O. Stress relaxing hyaluronic acid-collagen hydrogels promote cell spreading, fiber remodeling, and focal adhesion formation in 3D cell culture. *Biomaterials* **154**, 213–222 (2018).
13. Hong, Y. et al. A strongly adhesive hemostatic hydrogel for the repair of arterial and heart bleeds. *Nat. Commun.* **10**, 1–11 (2019).
14. Hozumi, T., Kageyama, T., Ohta, S., Fukuda, J. & Ito, T. Injectable hydrogel with slow degradability composed of gelatin and hyaluronic acid cross-linked by schiff's base formation. *Biomacromolecules* **19**, 288–297 (2018).
15. Blank, L. M., Hugenholtz, P. & Nielsen, L. K. Evolution of the hyaluronic acid synthesis (has) operon in Streptococcus zooepidemicus and other pathogenic streptococci. *J. Mol. Evol.* **67**, 13–22 (2008).
16. Prehm, P. Release of hyaluronate from eukaryotic cells. *Biochem. J* **267**, 185–189 (1990).
17. Day, A. J. & Prestwich, G. D. Hyaluronan-binding proteins: tying up the giant. *J. Biol. Chem.* **277**, 4585–4588 (2002).
18. Day, A. J. & De La Motte, C. A. Hyaluronan cross-linking: a protective mechanism in inflammation? *Trends Immunol.* **26**, 637–643 (2005).
19. Day, A. J. & Milner, C. M. TSG-6: a multifunctional protein with anti-inflammatory and tissue-protective properties. *Matrix Biol.* https://doi.org/10.1016/j.matbio.2018.01.011 (2018).
20. Burdick, J. A. & Prestwich, G. D. Hyaluronic acid hydrogels for biomedical applications. *Adv. Mater.* **23**, 41–56 (2011).
21. Highley, C. B., Prestwich, G. D. & Burdick, J. A. Recent advances in hyaluronic acid hydrogels for biomedical applications. *Curr. Opin. Biotechnol.* **40**, 35–40 (2016).
22. Ricard-Blum, S. & Vallet, S. D. Fragments generated upon extracellular matrix remodeling: Biological regulators and potential drugs. *Matrix Biol.* **75–76**, 170–189 (2019).
23. Bourhis, J. M. et al. Structural basis of fibrillar collagen trimerization and related genetic disorders. *Nat. Struct. Mol. Biol.* **19**, 1031–1037 (2012).
24. Yu, Z., An, B., Ramshaw, J. A. M. & Brodsky, B. Bacterial collagen-like proteins that form triple-helical structures. *J. Struct. Biol.* **186**, 451–461 (2014).
25. Kalson, N. S. et al. Nonmuscle myosin II powered transport of newly formed collagen fibrils at the plasma membrane. *Proc. Natl. Acad. Sci. USA* **110**, E4743–E4752 (2013).
26. Wang, H. et al. An in situ activity assay for lysyl oxidases. *Commun. Biol.* **4**, 840 (2021).
27. Frantz, C., Stewart, K. M. & Weaver, V. M. The extracellular matrix at a glance. *J. Cell Sci* **123**, 4195–4200 (2010).
28. Karamanos, N. K., Theocharis, A. D., Neill, T. & Iozzo, R. V. Matrix modeling and remodeling: A biological interplay regulating tissue homeostasis and diseases. *Matrix Biol* **75–76**, 1–11 (2019).
29. Verderio, E. A. M., Johnson, T. & Griffin, M. Tissue transglutaminase in normal and abnormal wound healing: review article. *Amino Acids* **26**, 387–404 (2004).
30. Tsujimoto, I., Moriya, K., Sakai, K., Dickneite, G. & Sakai, T. Critical role of factor XIII in the initial stages of carbon tetrachloride-induced adult liver remodeling. *Am. J. Pathol.* **179**, 3011–3019 (2011).
31. Deweid, L., Avrutina, O. & Kolmar, H. Microbial transglutaminase for biotechnological and biomedical engineering. *Biol. Chem* **400**, 257–274 (2018).
32. Takahara, M., Wakabayashi, R., Minamihata, K., Goto, M. & Kamiya, N. Primary amine-clustered DNA aptamer for DNA-protein conjugation catalyzed by microbial transglutaminase. *Bioconjug. Chem.* **28**, 2954–2961 (2017).
33. Takahara, M., Wakabayashi, R., Minamihata, K., Goto, M. & Kamiya, N. Design of lipid-protein conjugates using amphiphilic peptide substrates of microbial transglutaminase. *ACS Appl. Bio Mater* **1**, 1823–1829 (2018).
34. Greenfield, N. J. Using circular dichroism spectra to estimate protein secondary structure. *Nat. Protoc.* https://doi.org/10.1038/nprot.2006.202 (2007).
35. Day, A. J., Aplin, R. T. & Willis, A. C. Overexpression, purification, and refolding of link module from human TSG-6 in Escherichia coli: effect of temperature, media, and mutagenesis on lysine misincorporation at arginine AGA codons. *Protein Expr. Purif.* **8**, 1–16 (1996).
36. Ge, X., Chen, L., Li, D., Liu, R. & Ge, G. Estimation of non-constant variance in isothermal titration calorimetry using an ITC measurement model. *PLoS ONE* https://doi.org/10.1371/journal.pone.0244739 (2020).
37. Higman, V. A. et al. A refined model for the TSG-6 link module in complex with hyaluronan: Use of defined oligosaccharides to probe structure and function. *J. Biol. Chem.* **289**, 5619–5634 (2014).
38. Tanaka, Y., Tsuruda, Y., Nishi, M., Kamiya, N. & Goto, M. Exploring enzymatic catalysis at a solid surface: a case study with transglutaminase-mediated protein immobilization. *Org. Biomol. Chem.* **5**, 1764–1770 (2007).
39. Schense, J. C. & Hubbell, J. A. Cross-linking exogenous bifunctional peptides into fibrin gels with factor XIIIa. *Bioconjug. Chem.* **10**, 75–81 (1999).
40. Haug, I. J., Draget, K. I. & Smidsrød, O. Physical and rheological properties of fish gelatin compared to mammalian gelatin. *Food Hydrocoll.* **18**, 203–213 (2004).
41. Guimarães, C. F., Gasperini, L., Marques, A. P. & Reis, R. L. The stiffness of living tissues and its implications for tissue engineering. *Nat. Rev. Mater.* **5**, 351–370 (2020).
42. Mutsaers, S. E., Prêle, C. M. A., Pengelly, S. & Herrick, S. E. Mesothelial cells and peritoneal homeostasis. *Fertil. Steril.* **106**, 1018–1024 (2016).
43. Kohda, D. et al. Solution structure of the link module: A hyaluronan-binding domain involved in extracellular matrix stability and cell migration. *Cell* **86**, 767–775 (1996).
44. Hauser-Kawaguchi, A., Luyt, L. G. & Turley, E. Design of peptide mimetics to block pro-inflammatory functions of HA fragments. *Matrix Biol.* **78–79**, 346–356 (2019).
45. Blixt, O., Collins, B. E., Van den Nieuwenhof, I. M., Crocker, P. R. & Paulson, J. C. Sialoside specificity of the siglec family assessed using novel multivalent probes: Identification of potent inhibitors of myelin-associated glycoprotein. *J. Biol. Chem.* **278**, 31007–31019 (2003).
46. Liu, G. J., Jia, L. Y. & Xing, G. W. Probing sialidases or siglecs with sialic acid analogues, clusters and precursors. *Asian J. Org. Chem.* **9**, 42–52 (2020).
47. Tanabe, A. et al. Production and characterization of a novel site-specific-modifiable anti-OX40-receptor single-chain variable fragment for targeted drug delivery. *Biochem. Biophys. Res. Commun.* **496**, 614–620 (2018).
48. Mahoney, D. J. et al. Characterization of the interaction between tumor necrosis factor-stimulated gene-6 and heparin: implications for the inhibition of plasmin in extracellular matrix microenvironments. *J. Biol. Chem.* **280**, 27044–27055 (2005).
49. Gastinel, L. N. Galactosyltransferases: a structural overview of their function and reaction mechanisms. *Trends Glycosci. Glycotechnol.* **13**, 131–145 (2001).
50. Qi, J. et al. Enzymatic formation of an injectable hydrogel from a glycopeptide as a biomimetic scaffold for vascularization. *ACS Appl. Mater. Interfaces* **10**, 6180–6189 (2018).
51. Broguiere, N., Isenmann, L. & Zenobi-Wong, M. Novel enzymatically cross-linked hyaluronan hydrogels support the formation of 3D neuronal networks. *Biomaterials* **99**, 47–55 (2016).
52. Boon, C. H., Gribbon, P. M., Day, A. J. & Hardingham, T. E. Hyaluronan binding to Link module of TSG-6 and to G1 domain of aggrecan is differently regulated by pH. *J. Biol. Chem.* **283**, 32294–32301 (2008).

53. Ando, H. et al. Purification and characteristics of a novel transglutaminase derived from microorganisms. *Agric. Biol. Chem.* **53**, 2613–2617 (1989).
54. Cao, T. V., La, M., Getting, S. J., Day, A. J. & Perretti, M. Inhibitory effects of TSG-6 link module on leukocyte-endothelial cell interactions in vitro and in vivo. *Microcirculation* **11**, 615–624 (2004).
55. Park, J. I. et al. Antitumor therapy mediated by 5-fluorocytosine and a recombinant fusion protein containing TSG-6 hyaluronan binding domain and yeast cytosine deaminase. *Mol. Pharm.* **6**, 801–812 (2009).
56. Ghosh, J. G. et al. Long-acting protein drugs for the treatment of ocular diseases. *Nat. Commun.* **8**, 14837 (2017).
57. Laing, S. T. et al. Retinal and lens degeneration in new zealand white rabbits administered intravitreal TSG-6 link domain-rabbit FAb fusion proteins. *Toxicol. Pathol.* **49**, 634–646 (2021).
58. Drummond, S. P. et al. The recombinant Link module of human TSG-6 suppresses cartilage damage in models of osteoarthritis: a potential disease-modifying OA drug. *medRxiv* https://doi.org/10.1101/2021.03.23.21254102 (2021).
59. Grigoryan, B. et al. Multivascular networks and functional intravascular topologies within biocompatible hydrogels. *Science* **364**, 458–464 (2019).
60. Koffler, J. et al. Biomimetic 3D-printed scaffolds for spinal cord injury repair. *Nat. Med.* **25**, 263–269 (2019).
61. Rayani, K. et al. Binding of calcium and magnesium to human cardiac troponin C. *J. Biol. Chem.* **296**, 100350 (2021).
62. Blundell, C. D. et al. Determining the molecular basis for the pH-dependent interaction between the link module of human TSG-6 and hyaluronan. *J. Biol. Chem.* **282**, 12976–12988 (2007).
63. Wiseman, T., Williston, S., Brandts, J. F. & Lin, L. N. Rapid measurement of binding constants and heats of binding using a new titration calorimeter. *Anal. Biochem.* **179**, 131–137 (1989).
64. Cao, W. & De La Cruz, E. M. Quantitative full time course analysis of nonlinear enzyme cycling kinetics. *Sci. Rep.* **3**, 3–7 (2013).
65. Blundell, C. D. et al. The link module from ovulation- and inflammation-associated protein TSG-6 changes conformation on hyaluronan binding. *J. Biol. Chem.* **278**, 49261–49270 (2003).

Acknowledgements

We thank Denka Co. for supplying HA, Ajinomoto Co. Inc. for supplying MTG, and Nitta Gelatin Inc. for supplying fish gelatin. This work was supported by JSPS KAKENHI (grant numbers: 17K19006 and 21J12834); the Uehara Memorial Foundation; and the Leadership Development Program for PhD, The University of Tokyo, Japan.

Author contributions

M.O., A.T., S.O., S.N., K.T., and T.I. designed the study. M.O. performed the experiments. M.O. analyzed the data. M.O., A.T., S.O., S.N., and T.I. interpreted the data. M.O. wrote the first draft of the manuscript, which was then critically reviewed and revised by all authors. T.I. conceptualized the study and is responsible, as the corresponding author, for all data generated/analyzed in this study. All authors have approved the final version of the manuscript.

Competing interests

The authors declare no competing interests.

Additional information

Supplementary information The online version contains supplementary material available at https://doi.org/10.1038/s43246-022-00309-4.

Correspondence and requests for materials should be addressed to Taichi Ito.

Peer review information *Communications Materials* thanks the anonymous reviewers for their contribution to the peer review of this work. Primary Handling Editor: Steven Caliari and John Plummer. Peer reviewer reports are available.

Reprints and permission information is available at http://www.nature.com/reprints

Publisher's note Springer Nature remains neutral with regard to jurisdictional claims in published maps and institutional affiliations.